

## Detector KEDR Tagging System for Two-Photon Physics

V.M. Aulchenko<sup>a</sup>, S.E. Baru<sup>a</sup>, A.E. Bondar<sup>a</sup>, G. Ya. Kezerashvili<sup>a</sup>, V.A. Kiselev<sup>a</sup>, N. Yu. Muchnoi<sup>a</sup>, V.P. Nagaslaev<sup>a</sup>, A.I. Naumenkov<sup>a</sup>, S.A. Nikitin<sup>a</sup>, I. Ya. Protopopov<sup>a</sup>, L.V. Romanov<sup>a</sup>, D.N. Shatilov<sup>a</sup>, E.A. Simonov<sup>a</sup>, A.A. Tatarinov<sup>a</sup>,

<sup>a</sup>Budker Institute of Nuclear Physics

A special system to tag scattered electrons (TS) from  $\gamma\gamma$ -processes is described. The system is intended for the experiments with KEDR detector at the VEPP-4M storage ring. This system has a high detection efficiency and good invariant mass resolution. Also the results of Monte-Carlo study with GEANT program for the reaction  $e^+e^- \rightarrow e^+e^-\pi^+\pi^-$  are described. It is shown that such pions can be distinguished from muons from the reaction  $e^+e^- \rightarrow e^+e^-\mu^+\mu^-$  using the combined information from TS and KEDR coordinate system.

### 1. Introduction

This paper describes the Tagging System (TS) ([1]) to study  $\gamma\gamma$  physics at the VEPP-4M collider ([2]) with the general-purpose detector KEDR ([3]).  $\gamma\gamma$  interactions (see, for example, [4]) allow to investigate states inaccessible in the one-photon channel.

The diagram for these processes is shown in Fig. 1a. The electron and positron radiate virtual photons which produce a C-even state. The momentum  $P_{\gamma\gamma}$  and c.m.s. energy  $W_{\gamma\gamma}$  of this state can be expressed through the lost energies of the scattered electron and positron (below referred to as SE):  $\omega_1, \omega_2$ :

$$P_{\gamma\gamma} = \omega_2 - \omega_1; \quad W_{\gamma\gamma} = 4\omega_1\omega_2 \quad (1)$$

The energy spectrum of virtual photons resembles the bremsstrahlung one ( $\sim 1/\omega$ ) and the photons are emitted mainly at small angles with respect to the beam. The SE angles are related to the photon angles by momentum conservation and are also small. As the masses of the photons are  $q_{1,2}^2 \approx 2E_{1,2}E'_{1,2}(1 - \cos\theta_{1,2})$  where  $\theta_{1,2}$  are angles of SE, the photons are typically almost real.

So, because of the properties of the  $\gamma\gamma$ -processes, to attain the high double-tag detection efficiency one has to detect SE emitted from the interaction point at a zero angle.

The interesting problems that can be investigated with the help of such system are:

- Study of the total cross section  $\gamma\gamma \rightarrow$  hadrons at low  $Q^2$  for  $M_{\gamma\gamma}$  up to 4 GeV;
- Study of C-even resonances  $\eta, \eta', f_2, a_2, \eta_c, \chi_{c0}, \chi_{c2}$ ;
- Measurement of  $\Gamma_{\gamma\gamma}$  of candidates for exotic states:  $f_0(1370), f_0(1500), f_J(1710), f_J(2220), \pi_2(1670)$ ;

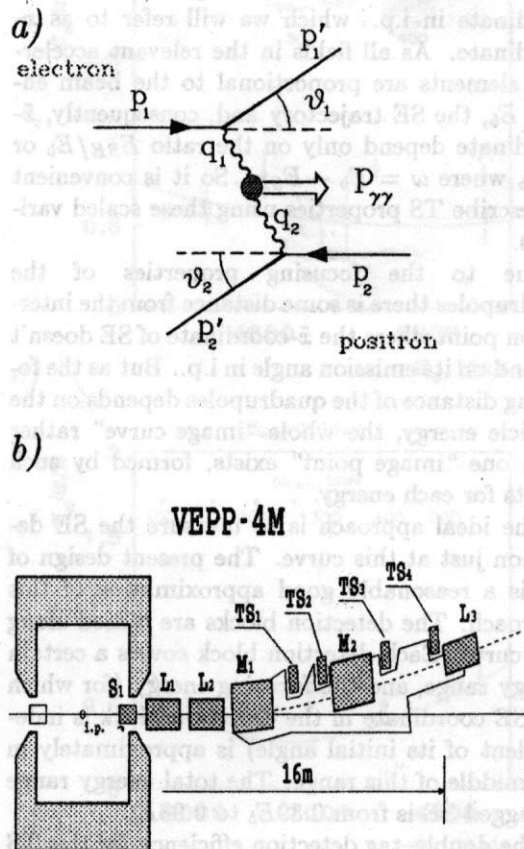


Figure 1. a) The diagram of the two-photon processes. b) Layout of VEPP-4M experimental region.

- Study of the cross section  $\gamma\gamma \rightarrow \pi\pi, K\bar{K}$  etc. close to threshold.

## 2. Tagging System design

The layout of the VEPP-4M experimental region together with TS is shown in Fig. 2b. The scattered electron (SE) emitted from the interaction point crosses quadrupole lenses  $L_1$  and  $L_2$ , bending magnets  $M_1$  and  $M_2$  and is detected by one of the four detection blocks  $TS_1 - TS_4$ . The symmetrical set-up is installed in the direction of the positron beam.

The SE deviation from the equilibrium orbit in the magnetic field is proportional to its energy loss, so one can calculate the SE energy losses using the transverse SE coordinate measured with the detection blocks. Let us denote this value  $\tilde{x}$ -coordinate to distinguish it from the coordinate in i.p. which we will refer to as  $x$ -coordinate. As all fields in the relevant accelerator elements are proportional to the beam energy  $E_b$ , the SE trajectory and, consequently,  $\tilde{x}$ -coordinate depend only on the ratio  $E_{SE}/E_b$  or  $\omega/E_b$  where  $\omega = E_b - E_{SE}$ . So it is convenient to describe TS properties using these scaled variables.

Due to the focusing properties of the quadrupoles there is some distance from the interaction point where the  $\tilde{x}$ -coordinate of SE doesn't depend on its emission angle in i.p.. But as the focusing distance of the quadrupoles depends on the particle energy, the whole "image curve" rather than one "image point" exists, formed by such points for each energy.

The ideal approach is to measure the SE deviation just at this curve. The present design of TS is a reasonably good approximation of this approach. The detection blocks are placed along this curve. Each detection block covers a certain energy range, and the focusing energy (for which the SE coordinate in the detection block is independent of its initial angle) is approximately in the middle of this range. The total energy range of tagged SE is from  $0.39E_b$  to  $0.98E_b$ .

The double-tag detection efficiency for this TS design for different beam energies is presented in Fig. 2a.

The detection blocks are designed as hodoscopes of drift tubes. The space resolution of the hodoscope is about  $300\mu\text{m}$ .

## 3. TS energy resolution

The basic limitations on the TS energy resolution arise from the energy, coordinate and angular spreads of the beam particles in the interaction

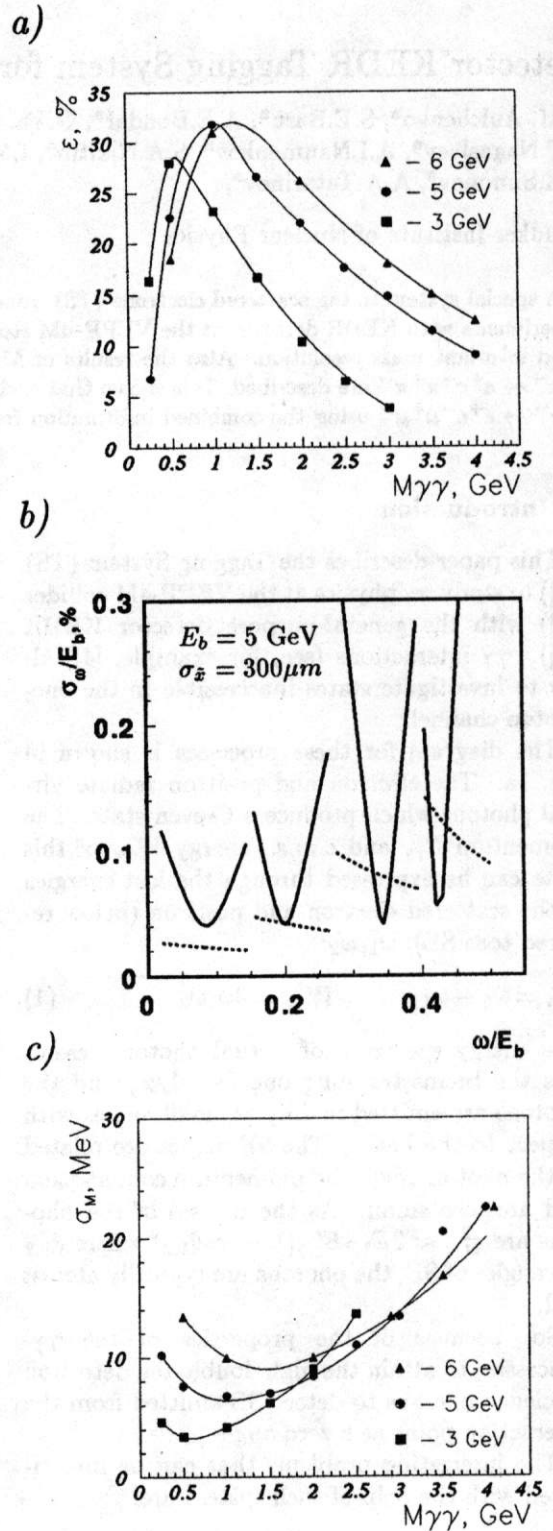


Figure 2. Tagging system properties: a) double-tag efficiency; b) energy resolution: the solid line is the contributions of the beam spreads, the dashed line is the contribution of the  $\sigma_{\tilde{x}} = 300\mu\text{m}$  space resolution of the detection blocks; c) The resolution over  $\gamma\gamma$  invariant mass.

point. These spreads smear the relation between SE deviation from the equilibrium orbit and its lost energy  $\omega_{SE}$ . To determine the TS energy resolution, one can simulate how SE with initial parameters distributed according to these spreads passes the accelerator structure. If  $\sigma_{\tilde{x}}^{beam}$  is the size of the coordinate distribution of SE with the fixed  $\omega_{SE}$  in the detection block, then the accelerator contribution to TS energy resolution for this  $\omega_{SE}$  is

$$\sigma_E^{beam} = \left( \frac{d\tilde{x}}{d\omega_{SE}} \right)^{-1} \sigma_{\tilde{x}}^{beam} \quad (2)$$

The results of such simulation are shown in Fig. 2b,c. Solid line in the Fig. 2b is the ratio of  $\sigma_E^{beam}$  to the beam energy  $E_b$  as a function of the  $\omega_{SE}/E_b$ . The dashed line at this picture shows the contribution of the coordinate resolution of the detection blocks which is equal to  $300\mu\text{m}$ . The resolution over  $W_{\gamma\gamma}$  is shown in Fig. 2c

For the experimental measurements of the TS energy resolution we use the process of the backward Compton scattering of the laser photons on the beam electrons. The special laser facility to produce the collision of the laser photons and beam electrons in the i.p. was designed for absolute energy calibration of TS ([1]). It includes the neodym (Nd:YAG) laser with the first harmonic energy 1.165 eV. The second harmonic with the energy 2.33 eV was also available. The special set-up of mirrors transports and focuses laser photons at i.p..

After interaction, photons move along the direction of the initial electron with angles of an order of  $1/\gamma$ , where  $\gamma$  is a relativistic factor for initial electrons. The maximum photon energy is

$$\omega_{max} = 4\gamma^2\omega_0 / (1 + 4\gamma\omega_0/m_e), \quad (3)$$

where  $\omega_0$  is the energy of the laser photon and  $m_e$  is electron mass. The natural width of the upper edge of these spectra which corresponds to the maximum energy loss, is negligible compared to the TS energy resolution, so the measured width of this edge gives the energy resolution of TS. The typical energy spectrum of the Compton photons measured with TS is shown in Fig. 3a.

The position of the Compton edge in TS is determined with  $\omega_{C,max}/E_b$  and depends on  $E_b$ . VEPP-4M can produce electrons with the beam energy from 0.9 GeV to 5.4 GeV. Thus, using the second laser harmonic one can measure the TS energy resolution and linearity in the whole range of the  $TS_4$  subsystem. The first harmonic allows to cover only about a half of the  $TS_4$  range, but in other combinations of  $E_b$  and  $\omega_{C,max}/E_b$ .

For the detailed study of the  $TS_4$  energy resolution in the wide range of  $E_b$  the Microstrip

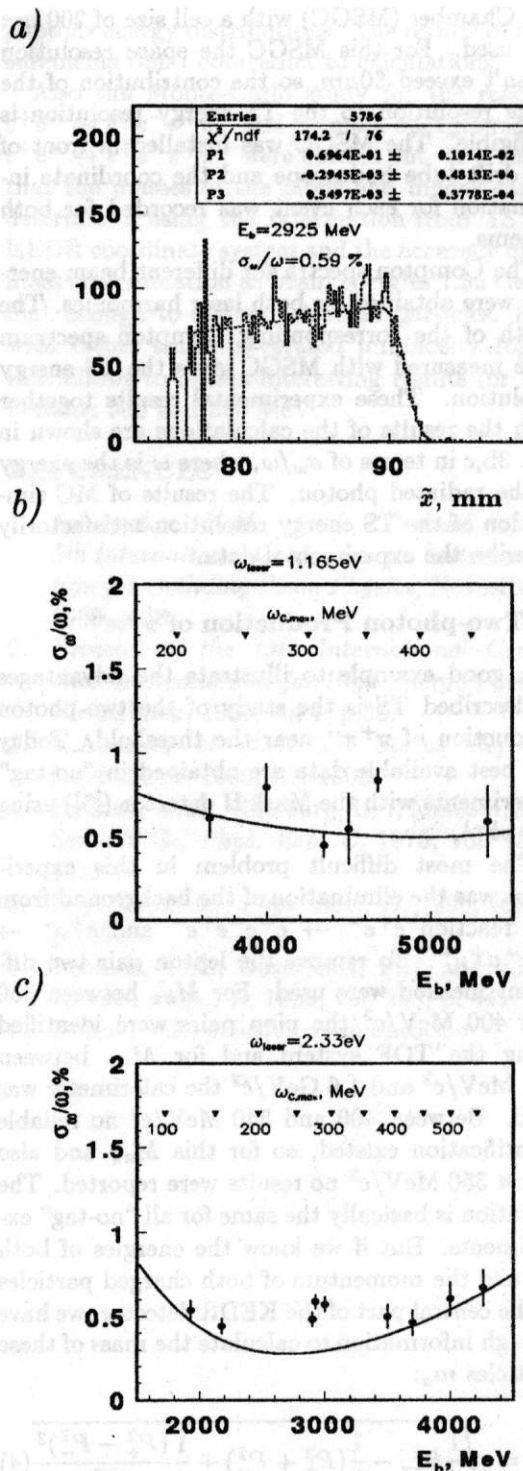


Figure 3. a) The example of the coordinate distribution of the Compton photon obtained using MSGC. The third fit parameter is the width of the spectrum edge in terms  $\sigma_\omega/E_b$ . b) and c) is the TS energy resolution measured with 1-st and 2-nd laser harmonic. Points are the measured TS energy resolution. The lines are the results of the MC calculations. Triangles show the Compton edge energies for corresponding beam energies.

Gas Chamber (MSGC) with a cell size of  $200 \mu m$  was used. For this MSGC the space resolution doesn't exceed  $60 \mu m$ , so the contribution of the space resolution to the TS energy resolution is negligible. The MSGC was installed in front of the drift tube hodoscope and the coordinate information for each event was recorded for both systems.

The Compton spectra for different beam energies were obtained for both laser harmonics. The width of the corresponding Compton spectrum edge measured with MSGC gives the TS energy resolution. These experimental results together with the results of the calculations are shown in Fig. 3b,c in terms of  $\sigma_\omega/\omega$ , where  $\omega$  is the energy of the radiated photon. The results of MC simulation of the TS energy resolution satisfactorily describe the experimental data.

#### 4. Two-photon Production of $\pi^+\pi^-$

A good example to illustrate the advantages of described TS is the study of the two-photon production of  $\pi^+\pi^-$  near the threshold. Today the best available data are obtained in "no-tag" experiments with the Mark II detector ([5]) using  $209 pb^{-1}$ .

The most difficult problem in this experiment was the elimination of the background from the reaction  $e^+e^- \rightarrow e^+e^-e^+e^-$  and  $e^+e^- \rightarrow e^+e^-\mu^+\mu^-$ . To remove the lepton pair two different methods were used. For  $M_{\pi\pi}$  between 350 and 400  $MeV/c^2$  the pion pairs were identified using the TOF system and for  $M_{\pi\pi}$  between 540  $MeV/c^2$  and 1.6  $GeV/c^2$  the calorimeter was used. Between 400 and 540  $MeV/c^2$  no reliable identification existed, so for this  $M_{\pi\pi}$  and also below 350  $MeV/c^2$  no results were reported. The situation is basically the same for all "no-tag" experiments. But if we know the energies of both SE and the momentum of both charged particles in the central part of the KEDR detector, we have enough information to calculate the mass of these particles  $m_x$ :

$$m_x = \sqrt{\frac{1}{4}E_{\gamma\gamma}^2 - \frac{1}{2}(P_+^2 + P_-^2) + \frac{1}{4}\frac{(P_+^2 - P_-^2)^2}{E_{\gamma\gamma}^2}} \quad (4)$$

Here  $E_{\gamma\gamma} = \omega_1 + \omega_2$  and  $P_+, P_-$  are the momenta of produced particles. If the accuracy is high enough, we can recognize pion and muon by their mass. This method can be called "kinematical identification".

At the first stage of experiments with KEDR detector it is planned to accumulate  $10 - 20 pb^{-1}$  in the  $J/\psi$  energy region. In order to check the possibilities which the kinematical identification

gives for investigation of  $e^+e^- \rightarrow e^+e^-\pi^+\pi^-$ , the detailed simulation of this process and  $e^+e^- \rightarrow e^+e^-\mu^+\mu^-$  was carried out using GEANT program.

As a generator for  $e^+e^- \rightarrow e^+e^-\mu^+\mu^-$  and  $e^+e^- \rightarrow e^+e^-\mu^+\mu^-\gamma$  the program of F.A.Berends [6] was used. The process  $e^+e^- \rightarrow e^+e^-\pi^+\pi^-$  was generated in Born approximation with program [7]. Of course for  $W_{\pi\pi} > \sim 550$  GeV the real cross-sections are much larger than Born production assumes due to the  $f_2(1270)$  resonance but even this approach is sufficient for the preliminary study near the reaction threshold which is the region of our prime interest. For both reactions the events with two reconstructed tracks in the KEDR coordinate system (drift chamber and vertex detector) and both SE registered in TS were selected. To describe the coordinate system response the current version of the KEDR full simulation and reconstruction was used. The preliminary TS simulation includes the relevant matter effects and the accelerator contributions to the TS energy resolution.

The results of the simulation for beam energy 1.55 GeV and integrated luminosity  $10 pb^{-1}$  are shown in Fig. 4. Figure 4a presents the  $\pi - \mu$  separation. The dashed line shows the separation with infinite TS resolution. It is seen, that approximately a half of the long tail of the muon distribution arises due to radiation of photons and other half is due to the SE interaction with the matter of in TS.

Figure 4b shows the number of  $e^+e^- \rightarrow e^+e^-\pi^+\pi^-$  events as a function of the  $W_{\pi\pi}$ . It is seen that even with such rather limited statistics we can fill the mentioned above  $W_{\pi\pi}$  gap in the MARK II cross-section measurements and obtain valuable results for  $W_{\pi\pi}$  in the range 300-400 MeV.

#### 5. Conclusions

The tagging system of the KEDR detector is able to measure the lost energy of the beam electrons scattered in the interaction point. The Compton scattering of laser photons at the beam electrons allows to obtain photons with energy up to 870 MeV. One can use the tagging system to determine the energy of these photons.

The energy resolution of the TS is of an order of 0.1% of the beam energy and depends on the beam energy and energy of radiated photon. The simple MC simulation which takes into account the accelerator structure and beam properties allows to calculate these dependences.

The tagging system energy resolution was obtained from the width of the edge of the Compton

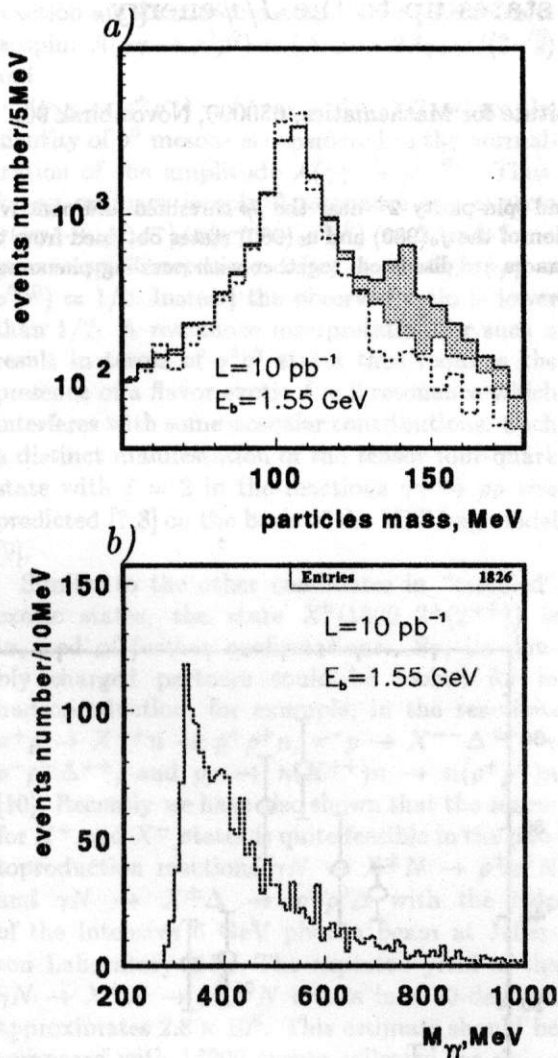


Figure 4. a) The solid line is the distribution over muon reconstructed masses for  $e^+e^- \rightarrow e^+e^-\mu^+\mu^-$  events, the shaded area shows the same distribution for  $e^+e^- \rightarrow e^+e^-\pi^+\pi^-$ , the dashed line is the muon mass distribution for the tagging system with absolute energy resolution. b) The distribution of the  $e^+e^- \rightarrow e^+e^-\pi^+\pi^-$  events over the  $\gamma\gamma$  invariant mass

photons energy distributions. The results of measurements don't contradict to calculations.

Also the Monte-Carlo study for the reaction  $e^+e^- \rightarrow e^+e^-\pi^+\pi^-$  and its main background are  $e^+e^- \rightarrow e^+e^-\pi^+\pi^-$  were carried out. It is shown that the masses of the pions and muons can be determined using the information from TS and KEDR coordinate system and the accuracy of the mass determination at beam energies 1.55 GeV is high enough to distinguish these particles. Even with rather small integrated luminosity  $10 \text{ pb}^{-1}$  that allows to obtain interesting results for  $W_{\pi\pi}$  between 300 and 550 MeV.

## REFERENCES

1. Aulchenko, V.M. et al., *Proceed. of the 5th International Conference on Instrumentation for Colliding Beam Physics*, Novosibirsk, 1990, p.68.
2. *Proceed. of the 13th International Conference on Accelerator for High Energy Particle*, Novosibirsk, 1986, vol.1, p.63.
3. V.Anashin et al., *KEDR Status Report*, Novosibirsk, 1990, RX-1308.
4. Budnev, V.M., Ginzburg, I.F., Meledin, G.V., Serbo, V.G., *Phys. Rep. C*, 1975, vol. 15, p. 181.
5. Boyer, J., et al., *Phys. Rev., D*, 1990, vol. 42, p.1350.
6. Berends, F.A., Daverfeldt, P.H. and Kleiss, R. *Nucl. Phys., B*, 1985, vol. 253, p. 441.
7. Telnov, V.I., *private communication*